Surface resonant levels in semiconductor superlattices

1990 J. Phys.: Condens. Matter 2 7137

(http://iopscience.iop.org/0953-8984/2/34/007)

J. Phys.: Condens. Matter 2 (1990) 7137–7142. Printed in the UK

Surface resonant levels in semiconductor superlattices

Yong S Joe and Sergio E Ulloa

Department of Physics and Astronomy, and Condensed Matter and Surface Sciences Program, Ohio University, Athens, OH 45701-2979, USA

Received 16 November 1989, in final form 21 February 1990

Abstract. Novel surface resonances in doped semiconductor superlattices are shown to exist in association with depletion regions. Self-consistent calculations in a tight-binding formalism for the electronic states of a GaAs–AlGaAs structure exhibit resonance-like states in high-energy minibands. These resonances extend throughout the superlattice, are strongly affected by applied electric fields, and are concurrent with significant changes in the local density of states. Calculated optical absorption curves show features related to surface resonances, making them accessible to experimental study.

Advances in the growth techniques of semiconducting materials controlled at the monolayer level have given rise to a great deal of research activity using semiconductor structures. This progress has allowed the observation of a variety of fundamental physical effects, as well as the realisation of new opto-electronic devices [1]. For example, semiconductor superlattices like those formed by alternating layers of GaAs–AlGaAs have recently been used to study such interesting physical questions as carrier localisation by electric fields [2], and the effects of controlled disorder on electronic properties [3]. In this paper we discuss the appearance of novel resonant states lying within the superlattice minibands. These resonances appear because of the potentials associated with inhomogeneous depletion charge regions at the end layers of doped superlattices, which alter the miniband scheme of an otherwise-periodic superlattice potential. One could view these resonant states as arising from the intrinsic surface-localised Stark levels of the system which become resonant with a higher miniband. The *surface resonances* are similar to levels introduced by impurities, such as resonances in metals [4], in semiconductors [5], or states associated with adsorbed atoms on metallic surfaces [6]. There are, however, important distinctions. The characteristic length scales in this case are provided by the rather large effective Bohr radius in these systems and by the structural parameters (layer thickness, alloy composition, etc). Moreover, the features of the resonant states presented here can be modified rather easily *for a given system* by the application of external electric fields that change the extent of the depletion regions. Such systems would then provide the unique ability to study resonant states *with readily controllable* experimental parameters, adding to the list of interesting physical problems that can be studied in semiconductor superlattice systems.

By growing thin layers of semiconductors with different band gaps, an effective electronic potential with the periodicity of the structure is introduced along the growth

0953-8984/90/347137+06$03.50

direction [1]. A prime example of these systems is a superlattice formed by layers of GaAs alternating with Si-doped layers of $Al_xGa_{1-x}As$ (which has a larger energy gap than GaAs). This structure can be visualised as the introduction of a modulation in the overall semiconductor lattice potential. This modulation can be varied by about 100 meV by changing the aluminium concentration x [7]. The resulting electronic levels for motion along the growth direction form a band structure which, by appropriate selection of the layer thicknesses, has tunable bandwidths and gaps, typically of a few meV.

The main features of this *miniband* structure are generally well understood in terms of simple Kronig–Penney models that use the as-designed layer thicknesses, as well as the strength of the potential barriers [1]. However, a realistic calculation of the electronic level structure in doped systems should include the effects of depletion regions arising from ever-present midgap defect states that produce Fermi level pinning [8,9]. The effects of depletion on *isolated* quantum-well levels can be understood in terms of a local potential that shifts the *independent* quantum well energies. However, because of the thin layers of the superlattice, the carriers tunnel between wells and a rearrangement of the charge occurs, yielding an inhomogeneous electronic density profile. Since this in turn affects the local potential and energy shifts, the calculation should be done in a *self-consistent* fashion.

A theory of resonant impurity states in solids has been developed in the literature [5,10]. However, the added complexity of the problem introduced by the self-consistent nature of the inhomogeneous potential requires a different formulation where the eigenstates of a *finite* system are calculated taking this self-consistent constraint into consideration. In this calculation the effective mass approximation is used for electronic motion within a given semiconductor layer. In addition, the degree of freedom in the perpendicular direction (the growth direction $\hat{x}$) is parametrised by a basis set of Wannier states ϕ_{js}, where $s(j)$ denotes the miniband (site) index. The corresponding envelope-function Hamiltonian, $H = H_{\|} + H_x$, can be described within a tight-binding approximation for H_x as [2]

$$H_x = \sum_{js}[(t_{os} + v_j)c_{js}^{\dagger}c_{js} + t_s c_{js}^{\dagger}c_{j+1,s} + t_s c_{j+1,s}^{\dagger}c_{js}] + \sum_{jss'} u_{jss'}c_{js}^{\dagger}c_{js'}. \tag{1}$$

Here, t_s is the hopping parameter for miniband s, $c_{js}^{\dagger}$ is the creation operator associated with ϕ_{js}, v_j is the inhomogeneous potential contribution to the local energy t_{os}, and $u_{jss'}$ represents the *potential-induced* miniband mixing [11]†. The potential is obtained by solving the Poisson equation with appropriate boundary conditions, taking into account the pinning of the Fermi level by the midgap states (at about 0.8 eV below the conduction band) which produces the inhomogeneous charge depletion. Consequently, the negative charge entering the Poisson equation is given by $\rho_j = (m/\pi\hbar^2)\sum_{\alpha s}|b_{js}^{\alpha}|^2(E_F - E_{\alpha})f_{\alpha}$, where f_{α} is the Fermi function. This completes the set of equations to be solved self-consistently; details for a similar calculation are given in [9]. This formulation is equivalent to a Hartree treatment of the inhomogeneous potential associated with the depletion regions.

† The miniband mixing term is estimated to be proportional to the potential gradient and the interminiband dipole matrix element, $u_{jss'} = (v_{j+1} - v_{j-1})d_{jss'}/2a$. The dipole matrix elements $d_{jss'} = \langle\phi_{js}|x|\phi_{js'}\rangle$ are calculated using explicit Wannier functions calculated numerically for the corresponding Kronig–Penney problem.

To illustrate the effects of miniband mixing introduced by the inhomogeneous potential, we have solved a two-miniband model with parameters corresponding to a GaAs–AlGaAs superlattice†. Further generalisation to include more minibands is straightforward, and the quantitative effects for the energy range considered here are negligible. Figure 1(*a*) shows the resulting level structure for a superlattice of thirty layers as one varies the donor doping density ρ_+ (variation of external electric fields would produce qualitatively similar results; see below). As expected, the level structure is composed of groups of levels corresponding to the minibands of a perfectly periodic superlattice. A downward tilting of the levels with respect to the fixed Fermi level for increasing ρ_+ is produced by the increasing total electron density. Notice also that a few levels appear detached from the minibands, in a degree which changes with ρ_+. These minigap-lying states have fairly localised wavefunctions near the end layers of the system, and are produced by the potential associated with the inhomogeneous charge depletion by defect states [9]. These surface-localised states can be understood as *intrinsic* Stark–Wannier states induced by the self-consistent charge depletion in the system. These states behave basically as superlattice Tamm states but with characteristic wavefunctions *extended over a few superlattice periods*, rather than on atomic scales.

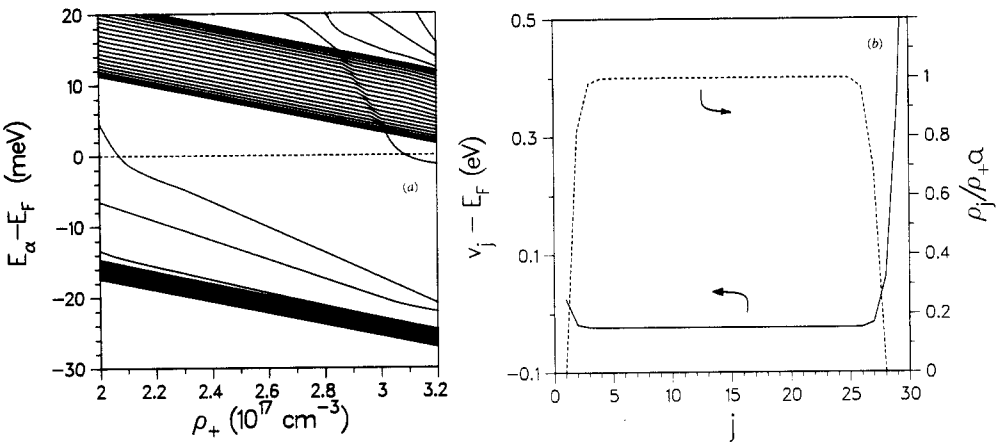

Figure 1. (*a*) Transverse-motion energy levels E_α for different doping densities ρ_+. The Fermi level is shown by the broken line. Notice level anticrossing and mixing in the upper miniband for $\rho_+ \approx 3$. (*b*) Resulting potential v_j, and charge density ρ_j for different layers j, for $\rho_+ = 2.95$. Notice charge depletion on both ends of superlattice.

Figure 1(*b*) shows sample results of the inhomogeneous potential v_j, and the electron charge density per layer ρ_j, for the case of $\rho_+ = 2.95 \times 10^{17}$ cm^{-3}. The charge depletion caused by the non-uniform potential is evident at both ends of the superlattice, where the effective potential is larger than in the middle layers [9].

It is most important for this paper to notice that in the neighbourhood of $\rho_+ \approx 3 \times 10^{17}$ cm^{-3}, one of the surface-localised states crosses the upper miniband.

† We use $t_1 = -0.62$ meV, $t_2 = 2.61$ meV, $t_{o1} = 0$, $t_{o2} = 32.6$ meV, $m = 0.067$, $\epsilon = 12.5$, $a = 226$Å, and $d_{j12}/a = 0.187$, which correspond approximately to a typical GaAs/$Al_xGa_{1-x}As$ superlattice with $x = 0.2$, and barrier width of 38Å. The superlattice is assumed to be grown on an undoped buffer layer 1100Å thick. These parameter values model a system such as that of [8].

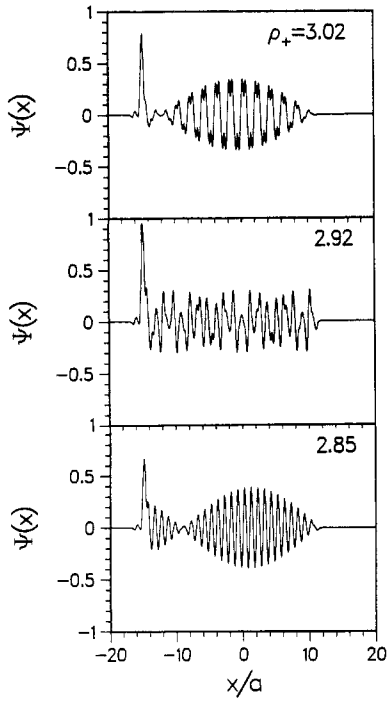

Figure 2. Wavefunctions for different doping densities (ρ_+ in units of 10^{17} cm^{-3}) corresponding to resonant eigenstate near top (ρ_+=2.85), middle (2.92), and bottom (3.02) of upper miniband in figure 1.

The anti-crossing behaviour exhibited there would suggest that mixing is taking place among nearly degenerate levels. This is indeed the case, as shown clearly in a plot of the corresponding eigenfunctions. Figure 2 shows selected transverse-motion eigenfunctions for different values of the doping density. A large-amplitude feature centred near the left end of the superlattice ($x/a \approx -15$) appears in these eigenstates as the doping density is varied, while they also have non-vanishing amplitudes all across the structure (which in this case extends from $x/a = -16$ to $+14$ in figure 2). This behaviour is in contrast to the midgap-lying surface states, which possess wavefunctions strictly localised to one or two superlattice periods. It is evident that strong mixing takes place whenever the structure parameters are such that a localised state (associated mostly with a low-energy miniband) is nearly degenerate with an upper miniband. This gives rise to eigenstates of combined localised–extended character. These mixed states are reminiscent of the resonant levels associated with impurities discussed in the literature [4–6], but are clearly produced by a totally different mechanism. Moreover, since the depletion region width is strongly affected by applied electric fields, so would the characteristics of the resonant levels. Indeed, one observes that the near-degeneracy conditions between a localised level and a miniband, needed for the resonance to develop, are easily shifted by small fields [12]. This change in properties would in turn have important observable consequences. It is to be expected, for example, that varying the localisation profile of the resonance would provide for different spectral weights in typical experiments such as optical absorption or Raman scattering [5, 13].

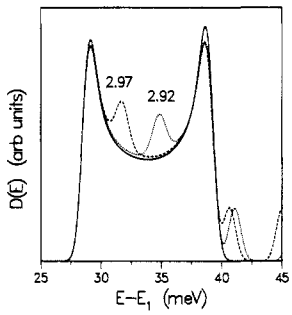

Figure 3. Density of states E_α measured with respect to E_1 near the upper miniband range for ρ_+=2.3 (full curve), 2.92 (dotted curve) and 2.97 (broken curve). Strong labelled features are surface-resonant states, absent for 2.3.

As occurs for typical resonances, the local density of states in these systems is perturbed when a surface resonance is present. This behaviour is also reflected by an enhanced density of transverse-motion states for energy values corresponding to the resonance, as shown in figure 3 for several values of the doping density. The energy range shown corresponds to the upper miniband in figure 1(*a*), and a Gaussian level broadening of 1 meV has been assumed. The strong labelled feature displayed by the density of states and produced by the resonance suggests possible important consequences in experiments. These resonant states also show in the total density of states, which includes the in-plane motion degrees of freedom, as additional features in the differential. As an example of an experimental probe that couples directly to the density of tunnelling states, we estimate the optical absorption in this energy range. We calculate the imaginary part of the dielectric function of the system in the long-wavelength regime, using the well known RPA expression for ϵ_2 [14]

$$\epsilon_2(\omega) = \frac{4\pi e^2 m}{Na\hbar^2\epsilon} \sum_{\alpha,\alpha'} |\, P_{\alpha\alpha'}\,|^2\, (E_F - E_\alpha) f_\alpha [g(E_{\alpha'} - E_\alpha - \hbar\omega) - g(E_{\alpha'} - E_\alpha + \hbar\omega)] \tag{2}$$

with $g(z) = (1/\gamma\sqrt{2\pi})\exp(-z^2/2\gamma^2)$, which takes into account level broadening effects, and where $P_{\alpha\alpha'} = \langle\alpha|x|\alpha'\rangle$ are the dipole matrix elements calculated using explicit Wannier functions [11]. Figure 4 shows results for two different doping densities, although different *electric fields* would yield the same qualitative results [9, 12]. The appearance of an additional absorption feature in the energy region corresponding to inter-miniband excitations ($\omega \approx 35$ meV) is both a reflection of the enhanced density of states and, most significantly, of variations in the optical matrix elements linking the miniband with the mixed resonant levels. These results would suggest experiments to study the existence and properties of surface-resonant states via far-infrared absorption [13]. Possible depolarisation effects have been neglected in this figure [15]. However, preliminary calculations including these effects indicate that the resonance features are still present and highly noticeable, although shifted slightly.

The strongly perturbed wavefunction associated with the resonances (figure 2) would also suggest that *tunnelling* experiments be used to study these. Since tunnelling coefficients for transport through a structure are extremely sensitive to phase coherence effects, it is anticipated that they would be strongly affected by the presence of a resonance like those described here. Ongoing calculations of this effect will be presented elsewhere.

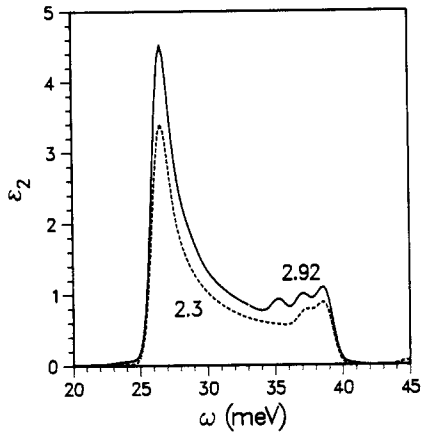

Figure 4. Imaginary part of dielectric function $\epsilon_2(\omega)$ in the region of interminiband absorption for ρ_+=2.92 (full curve) and 2.3 (broken curve). The extra feature at $\omega \approx 35$ meV arises from resonance-enhanced density of states in figure 3. The overall amplitude for 2.92 is larger, due to increased total charge.

Acknowledgments

We thank helpful discussions with G Kirczenow and J Zhang. Some of the calculations were performed on the Cray X-MP/28 at the Ohio Supercomputer Center. This work was supported by the US Department of Energy, grant no DE-FG02-87ER45334.

References

[1] Esaki L 1986 *IEEE J. Quantum Electron.* **22** 1611
Stiles P J 1988 *Interfaces, Quantum Wells and Superlattices (NATO ASI Series B, vol 179)* ed C R Leavens and R Taylor (New York: Plenum) p 1
[2] Mendez E E, Agulló-Rueda F and Hong J M 1988 *Phys. Rev. Lett.* **60** 2426
Bleuse J, Bastard G and Voisin P 1988 *Phys. Rev. Lett.* **60** 220
Austin E J and Jaros M 1987 *J. Appl. Phys.* **62** 558
[3] Das Sarma S, Kobayashi A and Prange R E 1986 *Phys. Rev. Lett.* **56** 1280
Chomette A, Deveaud B, Regreny A and Bastard G 1986 *Phys. Rev. Lett.* **57** 1464
[4] Doniach S and Sondheimer E H 1974 *Green's Functions for Solid State Physicists* (New York: Benjamin)
[5] Priester C, Allan G and Lannoo M 1984 *Phys. Rev.* B **29** 3408
Perry T A, Merlin R, Shanabrook B V and Comas J 1985 *Phys. Rev. Lett.* **54** 2623
[6] Gadzuk J W 1974 *Surf. Sci.* **43** 44
[7] Miller R C, Gossard A C, Kleinman D A and Munteau O 1984 *Phys. Rev.* B **29** 3740
Goossen K W, Lyon S A and Alavi K 1987 *Phys. Rev.* B **36** 9370
[8] Störmer H L, Eisenstein J P, Gossard A C, Wiegmann W and Baldwin K 1986 *Phys. Rev. Lett.* **56** 85
Ulloa S E and Kirczenow G 1988 *Phys. Rev.* B **37** 8337
[9] Zhang J and Ulloa S E 1988 *Phys. Rev.* B **38** 2063 1989 *Solid State Commun.* **71** 643
[10] Bassani F, Ladonisi G and Preziosi B 1974 *Rep. Prog. Phys.* **37** 1099
[11] Kohn W 1973 *Phys. Rev.* B **7** 4388
[12] Joe Y S and Ulloa S E 1990 unpublished
[13] Reeder A A, McCombe B D, Chambers F A and Devane G P 1988 *Phys. Rev.* B **38** 4318
[14] Ziman J M 1972 *Principles of the Theory of Solids* (Cambridge: Cambridge University Press)
[15] Dahl D A and Sham L J 1977 *Phys. Rev.* B **16** 651
Zhang J, Ulloa S E and Schaich W L 1990 *Phys. Rev.* B **41** 5467